



# Water management of proton exchange membrane fuel cell based on control of hydrogen pressure drop



Mancun Song, Pucheng Pei\*, Hongshan Zha, Huachi Xu

State Key Laboratory of Automotive Safety and Energy, Tsinghua University, Beijing 100084, China

## HIGHLIGHTS

- A two-level characteristic of hydrogen pressure drop is observed and analyzed.
- The flooding process can be divided into four periods.
- Growth rate of two levels is calculated which is significant for flooding alarm.
- The fuel cell is neither flooding nor dehydration in the moist section.

## ARTICLE INFO

### Article history:

Received 25 December 2013

Received in revised form

9 May 2014

Accepted 10 May 2014

Available online 29 May 2014

### Keywords:

Proton exchange membrane fuel cell

Water management

Hydrogen pressure drop

Hydrogen purge

Fault diagnosis

## ABSTRACT

Flooding experiments in various conditions are developed and the hydrogen pressure drop is investigated on a two-piece PEM fuel cell in this study. A two-level characteristic of hydrogen pressure drop is observed and analyzed in combination with water droplet accumulation in channels. Based on the characteristic, the flooding process can be divided into four continuous periods, which are the proper period, the humid period, the transitional period and the flooding period. The voltage shows the segmented tendency during these periods. Experimental results show that current and temperature have little influence on the growth rate of the two levels, while the effects of pressure and hydrogen stoichiometry are remarkable. The growth rate can be calculated through the channel dimensions and matches the experimental results well. Hydrogen purge is not a fundamental method to solve flooding. The end of the humid period should be the boundary before flooding. The moist section can be obtained in the beginning part of the humid period. In this section PEM fuel cell is neither flooding nor dehydration by adjusting the cell temperature, which is verified by two additional experiments. This water management is convenient and swift for PEM fuel cell applications and the fault diagnosis.

© 2014 Elsevier B.V. All rights reserved.

## 1. Introduction

Proton exchange membrane (PEM) fuel cells are envisioned to be the future choice for portable power equipments or transportation power systems. PEM fuel cells offer advantages to other energy converter types, including high energy efficiency and their ability of zero emission. Despite the remarkable progress in PEM fuel cell science and technology during the past decade, optimum water management has not been achieved so far. The membrane must be sufficiently hydrated for its conductivity, and the humidification of the fuel gas is necessary [1,2]. Too much water causes “flooding”, which reduces the transport rate of reactants and voltage output [3]. Serious flooding even results in local heat point

[4], corrosion of materials and erosion of catalyst [5]. Too little water causes “dehydration”, which increases the ionic resistance and makes membrane dry and crisp [6]. Thus water management is one of key issues for PEM fuel cell performance and durability.

Operation conditions, such as gas flow rate, humidification and current density, have influence on water management [7,8]. Design schemes, such as channel shape and character of porous medium, have influence on water management [9,10]. Complicated parameters make water management difficult. It is common to establish water management models [11,12], while the existing models are not accurate and universal enough. Statistical methods or neural networks can be introduced to water management [13], while a large number of sample data are required and the interpretability is lacking. Several electrochemical techniques are usable for identifying “issues” with dry or wet conditions. Electrochemical impedance spectroscopy is used by Canut et al. [14]. The cell's transient

\* Corresponding author. Tel./fax: +86 10 62788558.

E-mail address: [pchpei@mail.tsinghua.edu.cn](mailto:pchpei@mail.tsinghua.edu.cn) (P. Pei).

response after current interruption is proposed by Rubio et al. [15]. Nonlinear frequency response analysis of dehydration phenomena is investigated by Kadyk et al. [16]. A static DC–DC converter is introduced for humidification diagnosis by Hinaje et al. [17]. While more simple techniques are still needed especially for engineering applications. Parameter monitoring, such as voltage, pressure drop and ionic resistance, is the most direct method [18,19]. It is important for water management to simplify test equipments, determine control boundaries, and improve predictive ability.

Pressure drop is a key parameter to diagnose water content of PEM fuel cell. Despite the more water in cathode than that in anode due to generation and electro-osmotic drag, the hydrogen pressure drop is more suitable for water management. First of all, the thin membrane enhances the back diffusion [20], and the micro-porous layer on the cathode increases water removal from the cathode to the anode [21]. In addition, the relative humidity (RH) of humidified hydrogen is high to make membrane sufficiently hydrated. Finally, the low flow rate and high reaction consumption of hydrogen make it difficult to blow out water [22]. Therefore, hydrogen pressure drop is more sensitive to liquid water. It can reflect not only the water content but also the water influence of PEM fuel cell. It is appropriate to carry out water management based on hydrogen pressure drop.

In this paper, the characteristic of hydrogen pressure drop during flooding experiments was observed and analyzed, and the effects of current, temperature, pressure and hydrogen stoichiometry were discussed. The boundary to avoid flooding was defined and was also calculated through the channel dimensions. The water management strategy based on control of hydrogen pressure drop was verified to be effective.

2. Experiments

2.1. Fuel cell testing system

Fig. 1 shows a schematic diagram of the experimental setup used in this study. There were mass flow controllers, T-type thermocouples, pressure transducers, Hall current sensor to monitor and control the gas flow rate, temperature, pressure and current, respectively. The hydrogen pressure drop (DP) was monitored by a differential pressure sensor. The humidifiers were before fuel cell, and relative humidity was decided by the dew-point temperature. An electronic load was used to make the fuel cell operate at constant current mode.

An embedded water management module was developed for this study. The analog to digital function achieved all of the data acquisition. The digital to analog function controlled the gas flow

Table 1  
Operation conditions of flooding experiments.

Flooding experiment no.	Current/A	Temperature/K	Hydrogen pressure/kPa	Hydrogen stoichiometry
0-1	50	318	120	1.2
1-2	25			
1-3	75			
0-1	50	318	120	1.2
2-2		328		
2-3		313		
0-1	50	318	120	1.2
3-2			135	
3-3			150	
0-1	50	318	120	1.2
4-2				1.5
4-3				2.0

rate. The low side drive function adjusted the water temperature of both the coolant channels and the humidifiers. The serial interface achieved communication between the module and the computer. The microcontroller unit enabled all the functions by programming. The water temperature rose/declined by opening/closing the heaters and closing/opening the fans.

2.2. Fuel cell assembly

The two-piece fuel cell has 274 cm<sup>2</sup> active surface area assembled by two F881 epoxy glass end plates and two graphite plates with machined parallel flow fields. The flow fields have 1.0 mm channel width and 0.5 mm channel depth. Two golden-plated copper plates are employed to collect the current generated from the fuel cell. Two PTFE gaskets are used to seal the fuel cell as well as to protect the MEA from over-compression. The NafionR N112 MEAs are obtained from DuPont de Nemours and the Pt catalyst loading on the electrode is 0.3 mg cm<sup>−2</sup>. The rated temperature of the fuel cell is 328 K, and the maximum design pressure is 150 kPa.

2.3. Flooding experimental conditions

Flooding experiments in various conditions were carried out to observe the characteristic of hydrogen pressure drop during the flooding process. The operation conditions were shown in Table 1. Both of hydrogen and air were humidified to RH 100% in order to accelerate flooding. Four groups of contrast experiments were developed, and the contrastive parameters were current, temperature, hydrogen pressure and hydrogen stoichiometry. Air pressure was the same as hydrogen pressure and air stoichiometry was 2.0

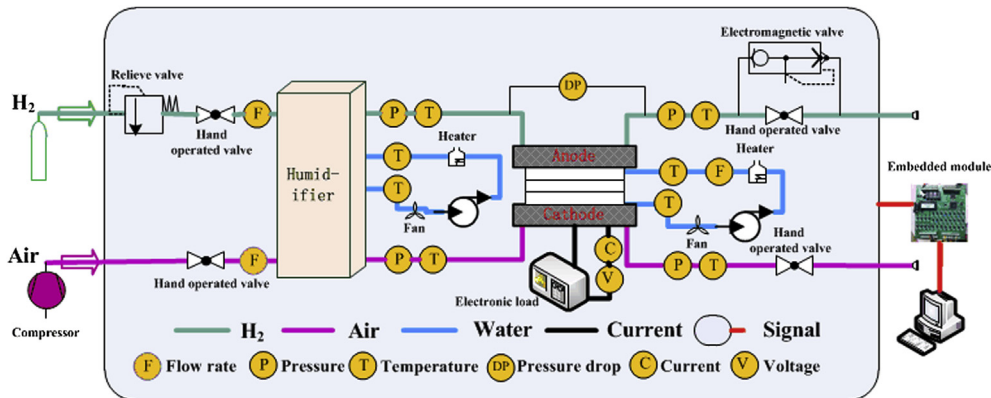
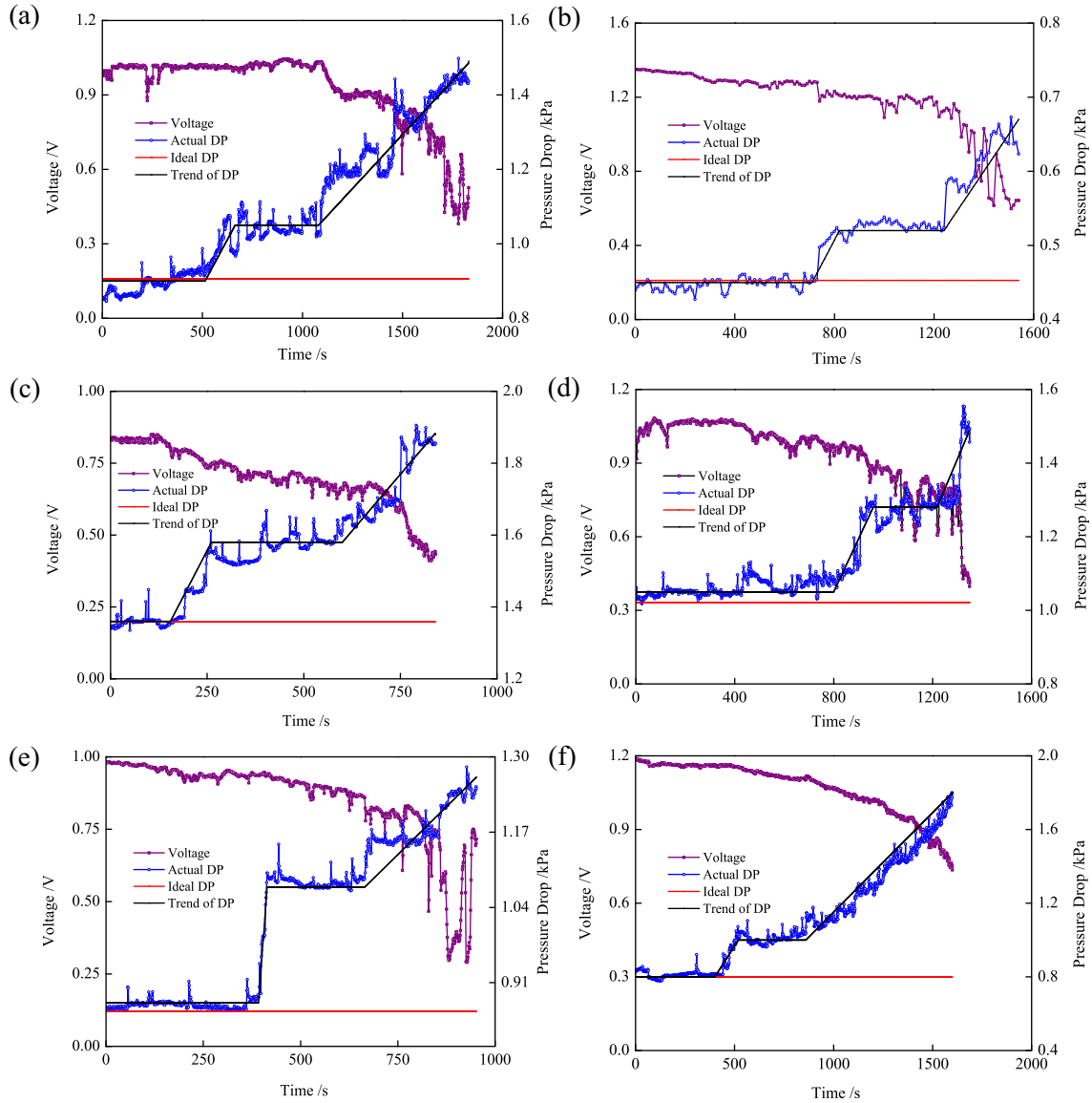


Fig. 1. Schematic diagram of the experimental setup used in this study.



**Fig. 2.** Voltage and hydrogen pressure drop results in flooding experiments numbered: (a) 0-1; (b) 1-2; (c) 1-3; (d) 2-2; (e) 2-3; (f) 3-2; (g) 3-3; (h) 4-2; (i) 4-3.

for constant. There were nine flooding experiments, which were numbered as shown in Table 1. During the experiments, the data of voltage and the hydrogen pressure drop was acquired in the sampling frequency of 128 Hz. A set of data was exported per second through the average calculation.

#### 2.4. Hydrogen purge process

As shown in Fig. 1, the pressure of the hydrogen was controlled by relieve valve unit before the fuel cell and the hand operated valve at the terminal of the gas pipe. The opening degree of the hand operated valve was carefully adjusted to stabilize the hydrogen pressure. The transient hydrogen purge process was realized by opening the electromagnetic valve which was in parallel with the hand operated valve [23]. The whole purge process lasted for 1 s. As the hydrogen purge process started, the outlet hydrogen pressure sharply decreased to normal pressure, leading to large pressure drop from the hydrogen inlet to outlet. The hydrogen flow rate increased obviously during the purge process, which produced a great effect to blow liquid water off. It is worth noting that the

purge process would cause pressure impact on membrane, so it should not be carried out frequently.

### 3. Results and discussion

#### 3.1. Two-level characteristic

As shown in Fig. 2, the voltage and the hydrogen pressure drop (DP) during the nine flooding experiments are recorded and drawn. The Ideal DP is calculated by Eq. (1) [24], where  $\Delta p_f$  is ideal DP without water in hydrogen channels,  $C_w$  is hydrogen channel width,  $C_d$  is hydrogen channel depth,  $L$  is hydrogen channel length,  $n$  is hydrogen channel number,  $T$  is cell temperature,  $p_{H_2}$  is hydrogen pressure,  $p_{sat}$  is saturated vapor partial pressure,  $\lambda_{H_2}$  is hydrogen stoichiometry, and  $I$  is current. All are SI units.

$$\Delta p_f = \frac{1.1748 \times 10^{-9} (C_w + C_d)^2 L e^{T/275.7} T}{n (C_w \cdot C_d)^3 (p_{H_2} - p_{sat}) p_{H_2}^{0.0263}} (\lambda_{H_2} - 0.5) I \quad (1)$$

(313 K < T ≤ 373 K)

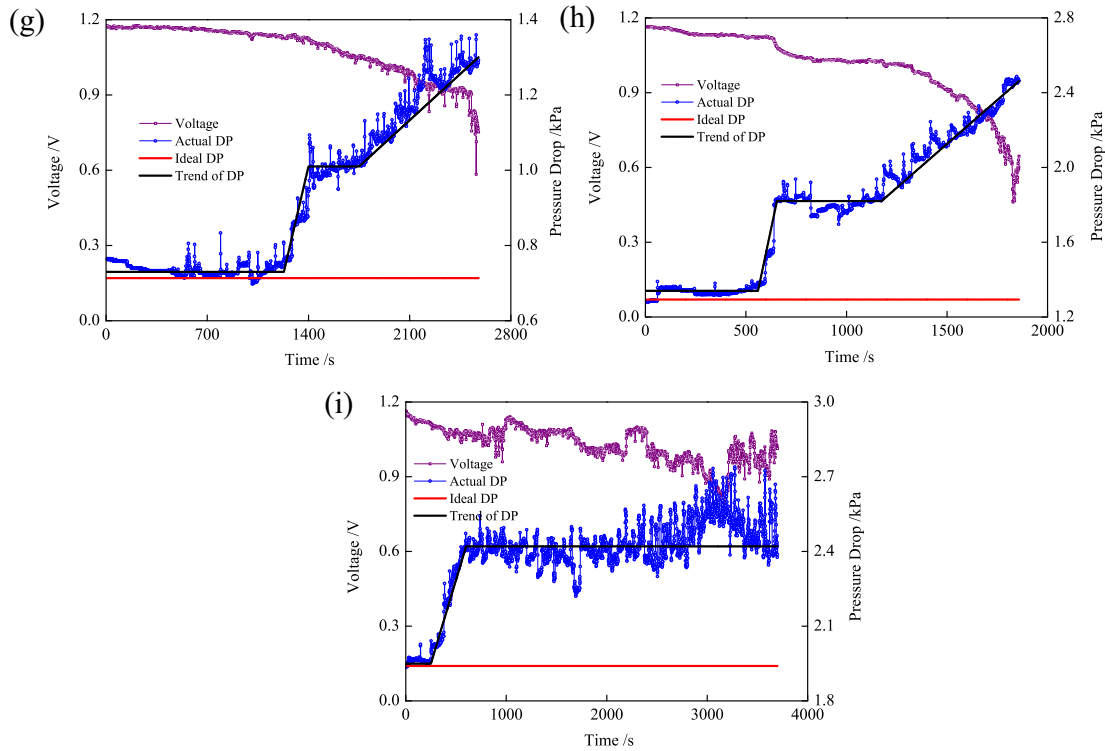


Fig. 2. (continued).

A two-level characteristic which includes two steady periods and two rising periods of hydrogen pressure drop is observed in the flooding process (except in the flooding experiment No. 4-3 which will be explained later). The trend of DP through least-square fitting is drawn in Fig. 2. The hydrogen pressure drop of the first level matches quite well with ideal DP.

There is often a two-phase flow in the channels of the PEM fuel cell. Many model and visualization researches have been carried out on the water formation, accumulation and transport [25]. The existing study has reported that two-phase flow in the channels occurs orderly in the form of droplet, film and slug-flow with the two-phase region being preceded by a single-phase region. A brief description of the different flow patterns as observed from channel images is given in Fig. 3 [26].

A significant discovery is that the two-level characteristic of hydrogen pressure drop corresponds to the flow patterns in Fig. 3. According to this, the flooding process can be divided into four continuous periods, which are the proper period, the humid period, the transitional period and the flooding period. Meanwhile, the voltage shows the segmented tendency during these periods.

- (1) Proper period corresponding to single-phase flow: Hardly any water droplets are observed in the channels and the flow is mostly in the form of gas. The actual DP is nearly the same as the ideal DP and keeps steady. The voltage is pretty high and constant.
- (2) Humid period corresponding to droplet flow: Water droplets emerge from underneath the GDL surface and remain adhered by surface tension forces. Due to the hydrophobic nature of carbon paper GDL surface, droplets are circular in shape and do not spread out laterally. As the droplets grow, the cross-sectional area of the channel decreases, which leads to the hydrogen pressure drop rising. On one hand, the accumulating water may humidify the membrane and promote the electrochemical reaction. On the other hand, the

performance of the fuel cell slightly declines because of the more and more water in GDL.

- (3) Transitional period corresponding to film flow: Further downstream, the influx of liquid water through GDL is sufficiently high so that the droplets, on contact either with neighboring droplets or channel walls, coalesce and are wicked into the walls and form a liquid film. The film coalesces with the droplets continuously and large droplets are no longer observed. The pressure drop keeps generally steady because of the film pattern of water, and the thickness of film is concerned with the channel dimensions and experimental conditions. In this period, the hydrogen transport is challenged by the amount of water, and there is a risk of voltage decline. The PEM fuel cell approaches flooding.
- (4) Flooding period corresponding to slug flow: Further growth of the film causes itself to accumulate into a slow-moving slug. This results in oscillations in the hydrogen pressure drop as stopping hydrogen flow through the channels. As the formation of slug flow, the voltage drops rapidly with fluctuation. The PEM fuel cell falls into flooding.

Moreover, there is almost film flow in the air channels under normal operation conditions because of the water generation and the high air flow rate. The whole two-level characteristic is infrequent and cannot be used to judge flooding simply.

### 3.2. Growth rate of two levels

The two-level characteristic is extremely important for flooding research, and the growth rate of the two levels ( $\phi_{DP}$ ) is defined as Eq. (2).

$$\phi_{DP} = \left( \frac{\text{DP of second level}}{\text{DP of first level}} - 1 \right) \times 100\% \quad (2)$$

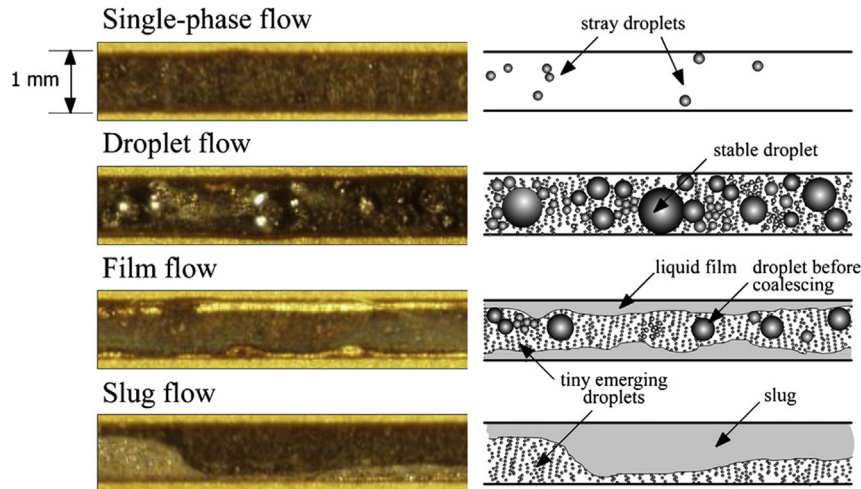


Fig. 3. Magnified view of flow patterns in channels and their corresponding line illustrations showing the form and distribution of liquid water [26].

The growth rates in the nine flooding experiments are shown in Table 2, and the effects of current, temperature, hydrogen pressure and stoichiometry can be discussed.

Current has hardly any effect on the growth rate, because the calculation of hydrogen pressure drop is proportional to the current and the effect can be eliminated.

Temperature has a little effect on the growth rate, because hydrogen is the major component in the vapor–hydrogen mixture in the suitable temperature for PEM fuel cell. In addition, there is a trade-off relationship between the increase of flow rate and vapor content with the increase of temperature.

Hydrogen pressure has a large effect on the growth rate. The growth rate increases obviously with the increase of hydrogen pressure. Pressure is a representation of energy to blow liquid water. Increasing pressure contributes to prevent fuel cell from flooding into flooding.

Hydrogen stoichiometry has noteworthy effect on the growth rate. Unlike the result of pressure, the growth rate decreases from 35.8% to 24.1% as the hydrogen stoichiometry increases from 1.5 to 2.0. It is concluded that the large hydrogen flow rate holds a remarkable ability to blow liquid water off and suppress the thickness of the film. That is why there is no slug flow in the flooding experiment 4-3, in which the pattern of two-phase flow is quite similar with that of air channels.

Although it can improve the ability of preventing flooding by increasing hydrogen pressure or stoichiometry, the system may be complex and power-wasting. Moreover, as shown in Fig. 4, the voltage drops dramatically as hydrogen stoichiometry from 2.0 to 1.2 in the transitional period of flooding experiment 4-3. This proves a large quantity of water in channels when the growth rate is high.

Table 2

The growth rate of hydrogen pressure drop in flooding experiments.

Flooding experiment no.	Growth rate/%
0-1	16.7
1-2	15.6
1-3	16.2
2-2	21.9
2-3	22.9
3-2	25.0
3-3	38.4
4-2	35.8
4-3	24.1

An extremely significant visualization has been carried out to research the droplet accumulation. It is validated that more and more droplets permeate through the GDL or the sidewall of channels, and the droplets grow large enough to coalesce with others. The average diameter of droplets which are about to coalesce is 0.33 mm in 1.5 mm width channels. The diameter has no relation with the channel depth because the coalescence happens on the surface of the GDL [27].

The similarity principle can be introduced and the average diameter of droplets is considered as 0.22 mm in the 1.0 mm width channels in this study. The coalescence of droplets leads the humid period to the transitional period. Fig. 5 shows the simplified droplet pattern in channel cross section at the end of the humid period.

The whole cross sectional area is:

$$A = 0.5 \times 1 = 0.5 \text{ mm}^2 \quad (3)$$

The area blocked by droplets is:

$$A_{\text{H}_2\text{O}} \approx 0.11 \times 1 \times \frac{\pi}{4} = 0.086 \text{ mm}^2 \quad (4)$$

The percent of blocked area is:

$$\frac{A_{\text{H}_2\text{O}}}{A} = \frac{0.086}{0.5} \times 100\% = 17.2\% \quad (5)$$

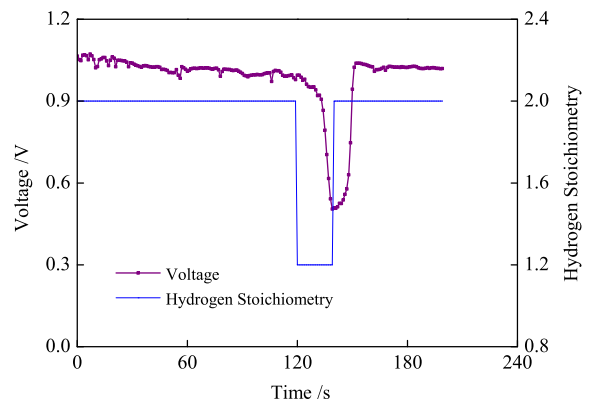


Fig. 4. Voltage responses as hydrogen stoichiometry changes in the transitional period of flooding experiment 4-3.

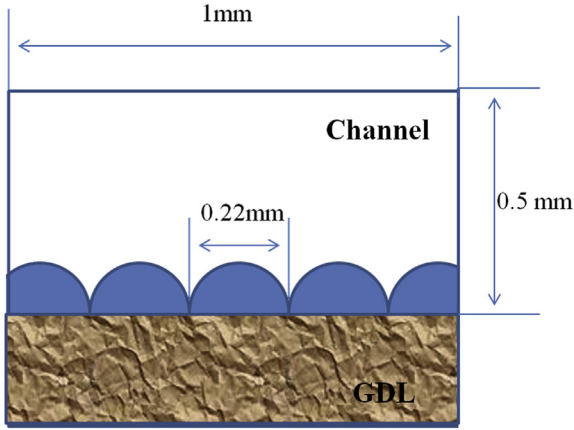


Fig. 5. Schematic diagram of the simplified droplet pattern in channel cross section at the end of humid period.

Because the pressure drop is about inversely proportional to the cross sectional area, the estimated value of the growth rate can be calculated as follows:

$$\dot{\phi}_{DP} = \frac{\frac{\Delta p_f}{1-17.2\%} - \Delta p_f}{\Delta p_f} \times 100\% = 20.8\% \quad (6)$$

The estimated growth rate matches quite well with that of experiments in usual conditions. Further on, the grow rate of the two levels can be calculated by the channel dimensions:

$$\dot{\phi}_{DP} \approx \frac{\frac{\Delta p_f}{1 - \frac{0.11 \times C_w \times C_w \times \pi/4}{C_w \times C_d}} - \Delta p_f}{\Delta p_f} = \frac{11\pi C_w}{400C_d - 11\pi C_w} \quad (7)$$

### 3.3. Effects of hydrogen purge

Hydrogen purge is a method to prevent fuel cell from falling into total flooding, and to recover the voltage. In order to investigate the effects of hydrogen purge, experiments in flooding period and transitional period are carried out.

As shown in Fig. 6(a), the hydrogen purge is taken in the flooding period of flooding experiment 2-2. Both of the hydrogen pressure drop and the voltage recover to the ideal value as the purge starts, which proves the ability of hydrogen purge to avoid flooding. As shown in Fig. 6(b), the hydrogen purge is taken in the transitional period of flooding experiment 4-3. The hydrogen

pressure drop lasts an extremely short time (about 10 s) before it return to the value before hydrogen purge. The voltage shows little change after purge. It is difficult to remove the water film in the transitional period by the shear force of gas and the hydrogen purge is less effective in this period [28].

The hydrogen purge is just a temporary method to avoid flooding. Flooding is quite easy to happen after the humid period. As a conclusion, the end of the humid period should be the boundary for fuel cell to avoid flooding, and the boundary of the hydrogen pressure drop for flooding alarm is:

$$\Delta p_{alarm} = (\dot{\phi}_{DP} + 1) \cdot \Delta p_f \quad (8)$$

### 3.4. The moist section (MS)

According to the results above, a moist section can be planned out of the humid period based on hydrogen pressure drop. In the research of literature [27], the humid period lasts for 50 min by taking analogy and in the first 25 min no coalescence happens. It means that the flooding needs not to be worried about in the first half of the humid period. On the other hand, dehydration might exist when the hydrogen pressure drop is nearly the ideal DP, because dehydration has no effect on the pressure drop. A feasible method is to make the actual DP slightly higher than the ideal DP, which indicates no dehydration from a certain extent.

Therefore, the moist section based on the hydrogen pressure drop can be limited as follows:

$$0 < \phi_{H_2} < \frac{\phi_{DP}}{2} \quad (9)$$

where  $\phi_{H_2}$  is define as follows:

$$\phi_{H_2} = \left( \frac{\text{Actual DP}}{\text{Ideal DP}} - 1 \right) \times 100\% \quad (10)$$

The range of the moist section should be less than the limits according to the actual requirements. In this study, the moist section is planned out as:

$$\phi_{H_2} \in [2.5\%, 7.5\%] \quad (11)$$

In the moist section, PEM fuel cell is supposed to be neither flooding nor dehydration, although a slight voltage reduction might happen because of water accumulation. The possible voltage reduction will not exceed 1% according to the results both in these flooding experiments and in the literature [27].

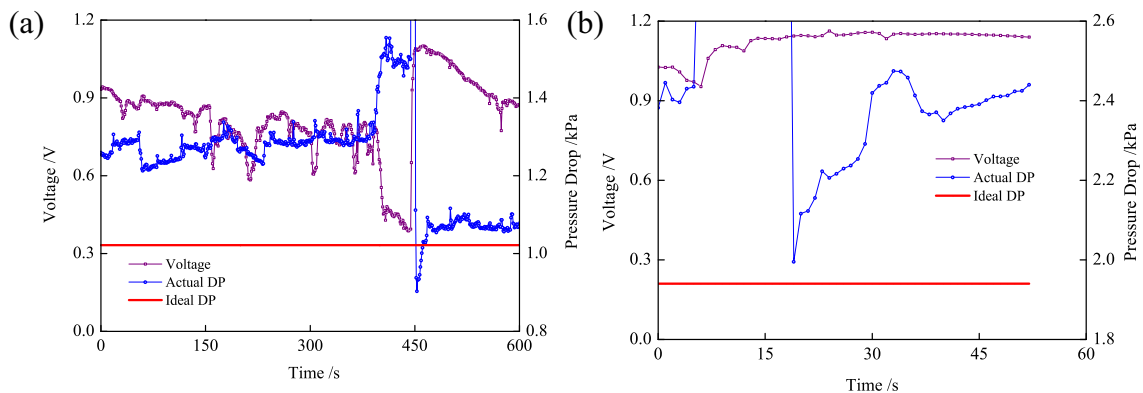


Fig. 6. The effects of the hydrogen purge (a) in flooding period of flooding experiment 2-2; (b) in transitional period of flooding experiment 4-3.

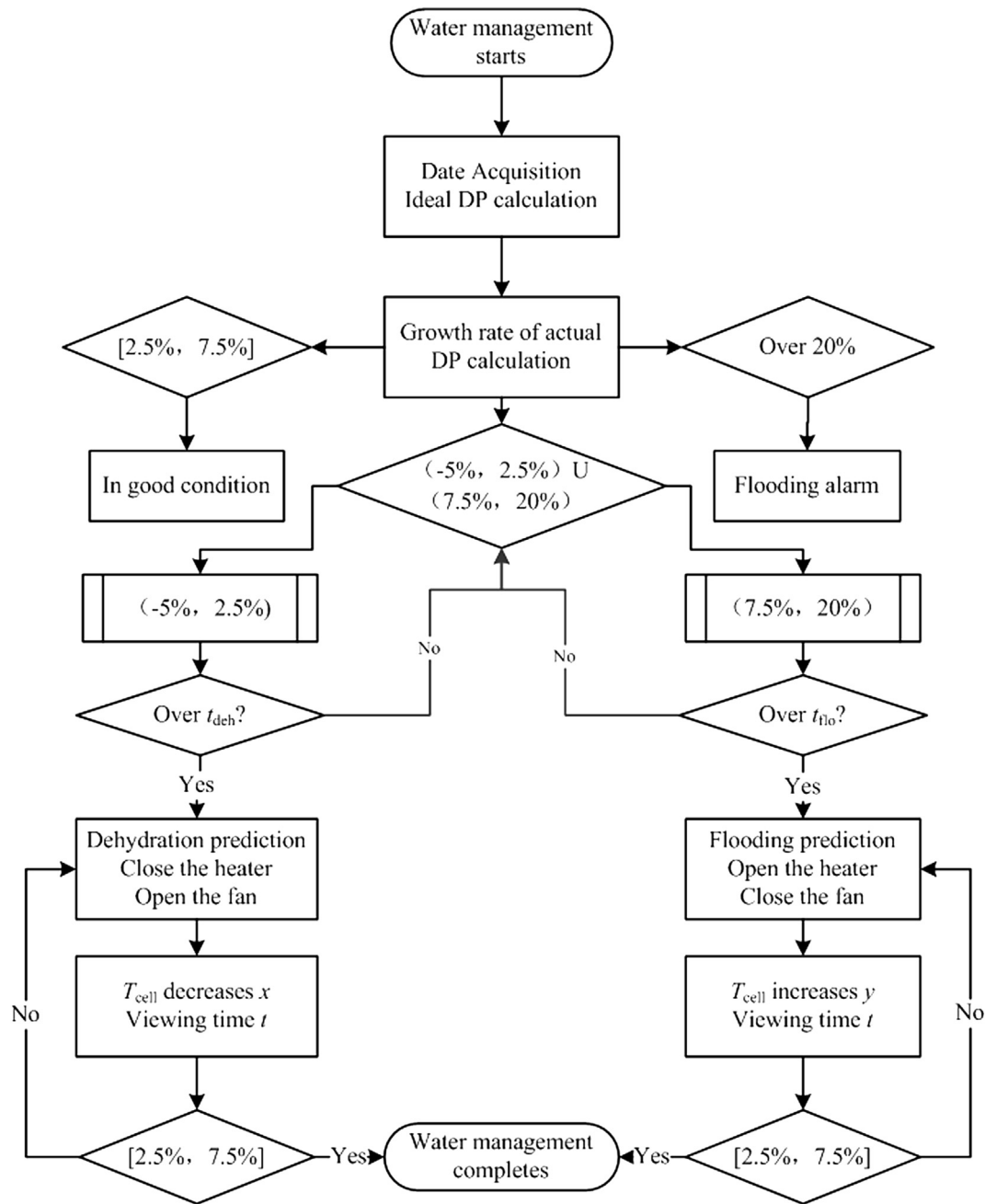


Fig. 7. The water management strategy by adjusting cell temperature based on hydrogen pressure drop.

### 3.5. Water management strategy and verification

As shown in Fig. 7, a water management strategy by adjusting the cell temperature is designed. There are two major advantages to adjust the cell temperature than to adjust the air humidification temperature. Firstly, the precision is improved because of the high heat dissipation of air. Secondly, the ideal DP moves by adjusting

the cell temperature which is more direct. Fig. 7 shows the water management in detail. The actual DP may a little lower than the ideal DP when the vapor–hydrogen mixture is unsaturated, so the lower limit of  $\phi_{H_2}$  is selected as  $-5\%$ .

In Fig. 7,  $x$  and  $y$  are the temperature drop and rise value,  $t$  is the viewing time,  $t_{deh}$  and  $t_{flo}$  are the judgment time of dehydration and flooding, respectively. Because flooding must be avoided while

Table 3

The initial conditions of two extreme experiments which are verification of the water management ability.

Experiment name	Current/A	Temperature/K	Pressure (C/A)/kPa	Stoichiometry (C/A)	Humidification temperature (C/A)/K
Extreme dehydration	50	330	120/120	2.0/1.2	318/318
Extreme flooding	75	318	120/120	2.0/1.2	323/323

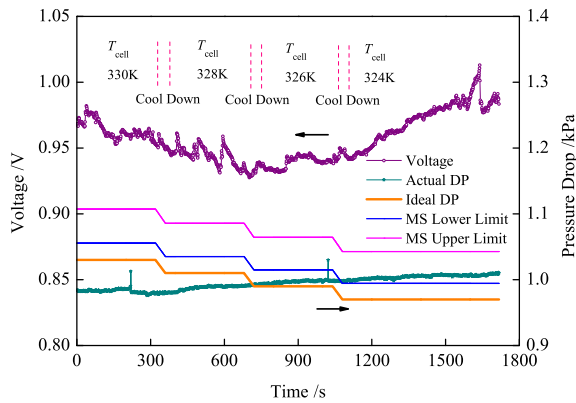


Fig. 8. The water management experiment to solve extreme dehydration.

dehydration can be accepted briefly, all the variables are planned as follows (SI units):

$$x = 2, \varphi_{H_2} \in [-5\%, 2.5\%] \quad (12)$$

$$y = \begin{cases} 5, \varphi_{H_2} \in [7.5\%, 15\%] \\ 8, \varphi_{H_2} \in [15\%, 20\%] \end{cases} \quad (13)$$

$$t = 300 \quad (14)$$

$$t_{\text{deh}} = 300 \quad (15)$$

$$t_{\text{flo}} = 60 \quad (16)$$

Two extreme experiments are designed to verify the water management ability to solve extreme dehydration and flooding, respectively. The fuel gas is quite dry in the beginning of the extreme dehydration experiment, while the fuel gas is supersaturated humidified in the beginning of the extreme flooding experiment. Moreover, the PEM fuel cell is out of operation for a long time before the extreme dehydration experiment to evaporate the water in it. The initial conditions of two experiments are shown in Table 3.

The result of the extreme dehydration experiment is shown in Fig. 8. At the beginning, the actual DP is lower than ideal DP which indicates the extreme dehydration. As the cell temperature decreases according to the water management strategy, the relative humidity of the hydrogen increases and the actual DP turns into the moist section through the lower limit. Meanwhile, the voltage turns to rise from decline gradually. Especially, the voltage is higher when

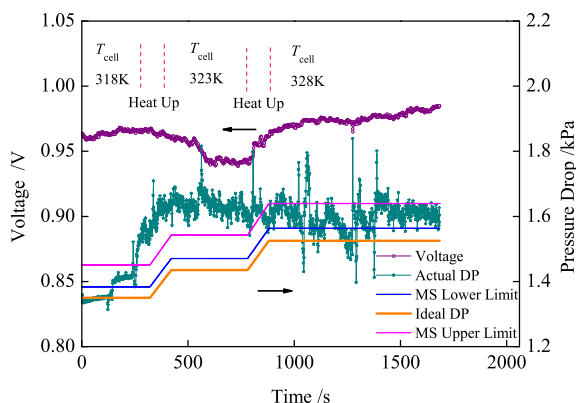


Fig. 9. The water management experiment to solve extreme flooding.

the hydrogen pressure drop is in the moist section. It verifies that the water management has the ability to prevent the PEM fuel cell from dehydration.

The result of the extreme flooding experiment is shown in Fig. 9. At the beginning period, there is a tendency of flooding and the actual DP exceeds the upper limit of the moist section. As the cell temperature increases, the hydrogen pressure drop is controlled in the moist section again, and the voltage turns to rise from decline gradually. The result verifies that the water management has the ability to prevent the PEM fuel cell from flooding. Therefore, the water management strategy is verified to successfully make the PEM fuel cell neither flooding nor dehydration.

#### 4. Conclusions

Flooding experiments are carried out and the hydrogen pressure drop and the voltage are investigated on a two-piece PEM fuel cell in this study. A two-level characteristic of the hydrogen pressure drop is observed during the flooding process. The flooding process is divided into four significative periods. The boundary before flooding is found out and is also calculated through the channel dimensions. A water management is carried out to make PEM fuel cell neither flooding nor dehydration. Comparing with the existing water management methods, this research finding presents a simple and specific standard to describe flooding process. Moreover, the water management strategy owns the excellent predictive ability to keep PEM fuel cell in good water conditions. The strategy can be easily used in engineering applications. And the water management based on hydrogen pressure drop conforms to the trend of the membrane thinner and thinner.

#### Acknowledgments

National Basic Research Program of China (973 Program) (2012CB215500), National High Technology Research and Development Program of China (863 Program) (2012AA110601) (2012AA053402), and National Natural Science Foundation of China (501100001809) (21376138) are gratefully acknowledged for funding this work.

#### References

- [1] G.H. Guveliogliu, H.G. Stenger, *J. Power Sources* 163 (2) (2007) 882–891.
- [2] Q.G. Yan, T. Hossein, J.X. Wu, *J. Power Sources* 158 (1) (2006) 316–325.
- [3] M. Najjari, F. Khemili, S.B. Nasrallah, *Renew. Energy* 33 (8) (2008) 1824–1831.
- [4] G.L. He, Y. Yamazaki, A. Abudula, *J. Power Sources* 194 (1) (2009) 190–198.
- [5] J. St-Pierre, D. Wilkinson, S. Knights, *J. New Mater. Electrochem. Syst.* 3 (2000) 99–106.
- [6] D.G. Sanchez, P.L. Garcia-Ybarra, *Int. J. Hydrogen Energy* 37 (2012) 7279–7288.
- [7] T. Ous, C. Arcoumanis, *J. Power Sources* 187 (1) (2009) 182–189.
- [8] F.B. Weng, Y. Su, C.Y. Hsu, *Int. J. Hydrogen Energy* 32 (6) (2007) 666–676.
- [9] J.P. Owejan, T.A. Trabold, D.L. Jacobson, M. Arif, S.G. Kandlikar, *Int. J. Hydrogen Energy* 32 (17) (2007) 4489–4502.
- [10] F.L. Chen, M.H. Chang, C.F. Fang, *J. Power Sources* 164 (2) (2007) 649–658.
- [11] A.Y. Karnik, A.G. Stefanopoulou, J. Sun, *J. Power Sources* 164 (2) (2007) 590–605.
- [12] M. Paquin, L.G. Frechette, *J. Power Sources* 180 (1) (2008) 440–451.
- [13] N.Y. Steiner, D. Hissel, P. Mocoteguy, D. Candusso, *Int. J. Hydrogen Energy* 36 (4) (2011) 3067–3075.
- [14] J.-M.L. Canut, R. Latham, W. Merida, D.A. Harrington, *J. Power Sources* 192 (2) (2009) 457–466.
- [15] M.A. Rubio, A. Urquia, S. Dormido, *J. Power Sources* 171 (2) (2007) 670–677.
- [16] T. Kadyk, R. Hanke-Rauschenbach, K. Sundmacher, *Int. J. Hydrogen Energy* 37 (9) (2012) 7689–7701.
- [17] M. Hinaje, I. Sadli, J.-P. Martin, P. Thounthong, S. Rael, B. Davat, *Int. J. Hydrogen Energy* 34 (6) (2009) 2718–2723.
- [18] H. Gorgun, M. Arcak, F. Barbir, *J. Power Sources* 157 (1) (2006) 389–394.
- [19] X. Liu, H. Guo, F. Ye, C.F. Ma, *Electrochim. Acta* 52 (11) (2007) 3607–3614.
- [20] G.J.M. Janssen, M.L.J. Overvelde, *J. Power Sources* 101 (1) (2001) 117–125.
- [21] D. Lee, J. Bae, *J. Power Sources* 191 (2) (2009) 390–399.

- [22] P.C. Pei, M.G. Ouyang, Q.C. Lu, H.Y. Huang, X.H. Li, *Int. J. Hydrogen Energy* 29 (10) (2004) 1000–1007.
- [23] J. Gou, P.C. Pei, Y. Wang, *J. Power Sources* 162 (2) (2006) 1104–1114.
- [24] P.C. Pei, M.G. Ouyang, W. Feng, L.G. Lu, H.Y. Huang, J.H. Zhang, *J. Hydrogen Energy* 31 (3) (2006) 371–377.
- [25] A. Bazylak, *J. Hydrogen Energy* 34 (9) (2009) 3845–3857.
- [26] I.S. Hussaini, C.Y. Wang, *J. Power Sources* 187 (2) (2009) 444–451.
- [27] T. Ous, C. Arcoumanis, *J. Power Sources* 173 (1) (2007) 137–148.
- [28] E.C. Kumbur, K.V. Sharp, M.M. Mench, *J. Power Sources* 161 (1) (2006) 333–345.